

# ChemComm

Accepted Manuscript



This is an *Accepted Manuscript*, which has been through the Royal Society of Chemistry peer review process and has been accepted for publication.

*Accepted Manuscripts* are published online shortly after acceptance, before technical editing, formatting and proof reading. Using this free service, authors can make their results available to the community, in citable form, before we publish the edited article. We will replace this *Accepted Manuscript* with the edited and formatted *Advance Article* as soon as it is available.

You can find more information about *Accepted Manuscripts* in the [Information for Authors](#).

Please note that technical editing may introduce minor changes to the text and/or graphics, which may alter content. The journal's standard [Terms & Conditions](#) and the [Ethical guidelines](#) still apply. In no event shall the Royal Society of Chemistry be held responsible for any errors or omissions in this *Accepted Manuscript* or any consequences arising from the use of any information it contains.

Cite this: DOI: 10.1039/c0xx00000x

www.rsc.org/chemcomm

COMMUNICATION

# Synthesis of Trapezohedral Indium Oxide Nanoparticles with High-Index {211} Facets and High Gas Sensing Activity

Xiguang Han,<sup>\*a</sup> Xiao Han,<sup>a</sup> Linqiang Sun,<sup>a</sup> Shengguang Gao,<sup>a</sup> Liang, Li,<sup>a</sup> Qin Kuang,<sup>b</sup> Zhaoxiong Xie<sup>\*b</sup> Chao Wang<sup>a</sup>

<sup>5</sup> Received (in XXX, XXX) Xth XXXXXXXXX 2014, Accepted Xth XXXXXXXXX 2014

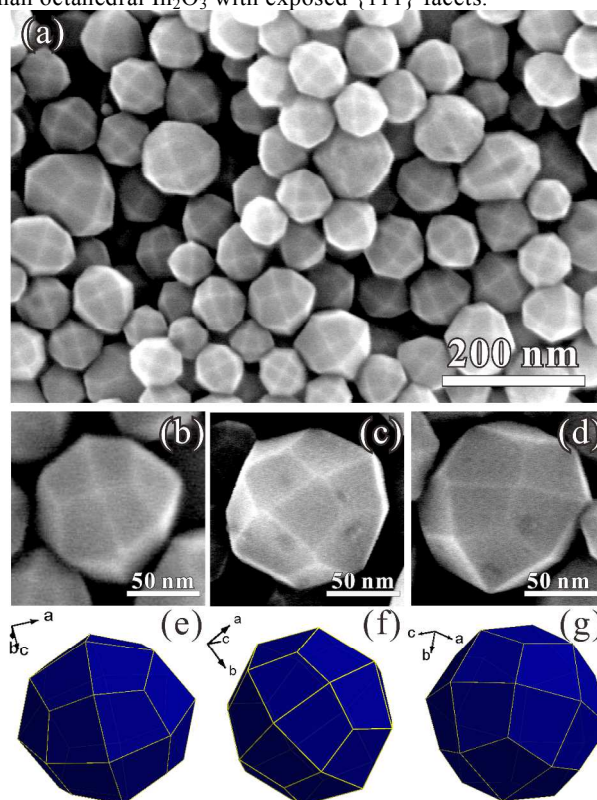
DOI: 10.1039/b000000x

Nanocrystals with high-index facets usually exhibit higher catalytic activities than those with only low-index facet. The trapezohedraon-shaped (TS)  $\text{In}_2\text{O}_3$  particles with exposed high-index {211} facets were successfully synthesized in oleic acid (OA) and trioctylamine (TOA) system. It has been demonstrated that the gas sensing activity of TS  $\text{In}_2\text{O}_3$  particles with exposed high-index {211} facets is higher than that of octahedron-shaped  $\text{In}_2\text{O}_3$  particles with exposed low-index {111} facets.

Anisotropy is the basic property for crystals, which results in different physical and chemical properties on various crystal facets or directions.<sup>[1]</sup> Particularly, the functional nanocrystals (NCs) with high-index facets generally exhibit higher chemical activities than those with only low-index facet, because the high-index facets have a high density of atomic steps, ledges, and kinks, which usually serve as active sites in chemical reactions.<sup>[2]</sup> For example, it has been demonstrated that  $\text{SnO}_2$  nanocrystals with (221) high index facets exhibit much better gas sensing properties toward alcohol than that of (110) surfaces with lower surface energy.<sup>[2i]</sup> Unfortunately, it is rather difficult to synthesize functional NCs that are enclosed by high-index facets of high surface energy, because crystal growth rates in the direction perpendicular to a high-index plane are usually much faster than those along the normal direction of a low-index plane and high-index planes are rapidly eliminated during crystal growth. During the past decade, a variety of face-centered cube structured metal NCs with high-index facets have been synthesized by different synthesized methods.<sup>[2a-i]</sup> However, compared with metal elements, metal oxides with high-index surfaces exposed are less reported, which could be due to

strong metal oxygen bonds.<sup>[2j-q]</sup>

Indium oxide ( $\text{In}_2\text{O}_3$ ), an n-type semiconductor with a bandgap of about 3.6 eV, has been widely applied in various areas, including biosensing,<sup>[3]</sup> nanoelectronics,<sup>[4]</sup> ultrasensitive gas sensors.<sup>[5]</sup> Up to date,  $\text{In}_2\text{O}_3$  nanomaterials with various morphologies such as nanobelt, nanowire, nanocube and nanooctahedron, have been synthesized via different synthesized methods.<sup>[6]</sup> However, the prepared  $\text{In}_2\text{O}_3$  nanocrystals are enclosed by {111} and {100} facets with low-index facets. In this communication, we firstly report a simple method for the preparation of trapezohedraon-shaped (TS)  $\text{In}_2\text{O}_3$  with exposed high-index {211} facets by exploiting the adsorption effect of oleic acid and trioctylamine at the temperature of 320 °C. The TS  $\text{In}_2\text{O}_3$  with exposed high-index {211} facets exhibit higher gas sensing activity than octahedral  $\text{In}_2\text{O}_3$  with exposed {111} facets.



<sup>a</sup>Jiangsu Key Laboratory of Green Synthetic Chemistry for Functional Materials, Department of Chemistry, School of Chemistry and Chemical Engineering, Jiangsu Normal University, Xuzhou, 221116 (P. R. China) E-mail: xghan@jsnu.edu.cn

<sup>b</sup>State Key Laboratory of Physical Chemistry of Solid Surfaces & Department of Chemistry, College of Chemistry and Chemical Engineering, Xiamen University, Xiamen 361005, China

† Electronic Supplementary Information (ESI) available. Detailed synthesis procedure and some experimental results see DOI: 10.1039/b000000x.

**Fig. 1** (a) SEM images of the TS  $\text{In}_2\text{O}_3$  NCs, (b-d) the high-magnification SEM images of individual polyhedron projected from different zone axis, (e-g) the ideal TS model enclosed by 24  $\{211\}$  facets projected from the corresponding zone axis to the (b-d).

Fig. 1a shows a representative SEM image of the as-prepared product, which is a pure cubic phase of  $\text{In}_2\text{O}_3$  as confirmed by the X-ray diffraction pattern (XRD) (Fig. S1). The images show that the majority (>90%) of the sample was TS NCs with size distribution mainly in the range of 70 – 120 nm (Fig. S2). The ideal TS models enclosed by 24  $\{211\}$  facets projected from different directions (Fig. 1e-g) match well with the synthesized NCs project from the same directions (Fig. 1b-d).

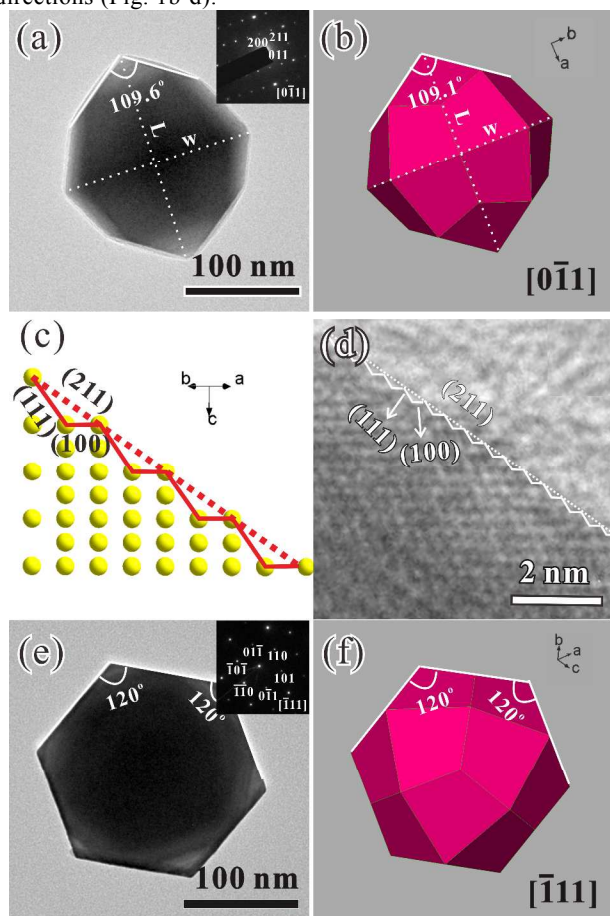


**Fig. 2** (a) TEM image of an individual TS  $\text{In}_2\text{O}_3$  NC projected from  $[0\bar{1}1]$  direction, where the top-right inset shows corresponding SAED pattern. (b) Schematic model of an ideal TS enclosed within  $\{211\}$  facets viewed along the  $[0\bar{1}1]$  direction, (c) Atomic model of the  $\{211\}$  surface of a NC, projected from the  $[0\bar{1}1]$  direction, showing that the  $\{211\}$  surface can be thought of as a combination of (111) terraces and (100) steps, (d) HRTEM image taken from the TS  $\text{In}_2\text{O}_3$  NCs, (e) TEM image of the same TS  $\text{In}_2\text{O}_3$  particle viewed along  $[\bar{1}11]$  direction, inset: the corresponding SAED pattern, (f) schematic model of an ideal TS enclosed within  $\{211\}$  facets viewed along the  $[\bar{1}11]$  direction.

In order to further confirm the structural information of the TS  $\text{In}_2\text{O}_3$  particle, the products were characterized by transmission electron microscopy (TEM). Fig. 2a shows a low-magnification TEM image of an individual TS particle, where the inset is the corresponding selected-area electron diffraction (SAED) pattern. The SAED pattern can be indexed to the  $[0\bar{1}1]$  zone axis of cubic  $\text{In}_2\text{O}_3$ , which implies that the

as-prepared TS  $\text{In}_2\text{O}_3$  particles are single-crystalline. Under electron-beam irradiation, the particle presents a diamond-like outline with a length/width ratio of about 1.1, and an apex angle between two side surfaces of about  $109.6^\circ$ . These structural features agrees well with the model of TS  $\text{In}_2\text{O}_3$  model with exposed  $\{211\}$  facets projected along the  $[0\bar{1}1]$  zone axis (Fig. 2b). Structurally,  $\{211\}$  surface can be described as combination of  $\{111\}$  terraces and  $\{100\}$  steps (Fig. 2c). In fact, such a stepped surface composed of  $\{111\}$  terraces and (100) steps can be directly captured in high-resolution TEM (HRTEM) images of the TS (Fig. 2d). To further confirm the exposed surfaces of the TS  $\text{In}_2\text{O}_3$ , the same particle was rotated to the  $[\bar{1}11]$  zone axis. As shown in Fig. 2e and f, both the outline and the apex angle of the particle still match well with the TS  $\text{In}_2\text{O}_3$  model enclosed by  $\{211\}$  facets, projected along the same direction (Fig. 2f). On the basis of the above TEM observations and structural analysis, we conclude that the exposed surfaces of the as-prepared TS  $\text{In}_2\text{O}_3$  particles are the  $\{211\}$  facets.

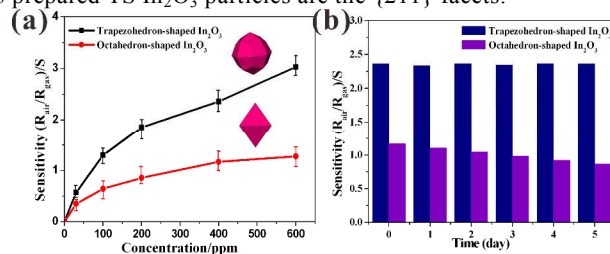


**Fig. 3** (a) Normalized sensitivity curves of  $\text{In}_2\text{O}_3$  particles of different shapes as a function of ethanol concentration per unit surface area.  $R$ = resistance, (b) The sensor response to 400 ppm ethanol at  $350^\circ\text{C}$  for five days.

During crystal growth, the high-index surfaces usually appear as growing facets because of their high surface energies and exhibit small facets or even disappear. Tuning the surface energy of specific crystal facet is an effective way to expose those high energy facets on the surface of crystallites. For example, growth of metal oxides in molten salt or ionic liquid benefits the formation of polar surface with high surface energy due to the electrostatic interaction. In our previous study, we found that a mixture of oleic acid (OA) and trioctylamine (TOA) can be thought as one kind of ionic liquid ( $\text{R-COOH} + \text{R-NH}_2 \rightarrow \text{R-COO}^- + \text{R-NH}_3^+$ ), by which ZnO hexagonal pyramid with whole polar surfaces were successfully prepared.<sup>[7]</sup> The as-prepared  $\text{In}_2\text{O}_3$  is in-centered cubic structure with a space group of  $Ia\bar{3}$ . From the crystal structure, it can be found (111) and (100) are polar surfaces with either negatively charged  $\text{O}^{2-}$  or positively charged  $\text{In}^{3+}$  ions, while (110) surfaces are nonpolar with neutral charge. When growing  $\text{In}_2\text{O}_3$  in the mixture of oleic acid (OA) and trioctylamine (TOA), polar surfaces should be preferred as demonstrated by the case of ZnO. Therefore, it is reasonable to form high-index (211) facets consisting of polar (111) and (100) subfacets. It should be note although both (111) and (100) surfaces are polar, the excess charge on (100) surface is larger than that on (111) surface. When increasing the reaction temperature, the electrostatic interaction could be weakened because of the thermo motion of ions. As a result, less polar (111) surface are preferred at high reaction temperature. As

evidence, we found octahedral  $\text{In}_2\text{O}_3$  NCs fully enclosed by (111) facets were found when the reaction temperature was increased to 360 °C (Fig. S3c, Fig. S4). To further demonstrate the ionic liquid effect, thermal decomposition of indium acetate in pure TOA and pure OA was carried out. When using pure OA, no products were obtained. According to our knowledge, the indium acetate has been dissolved by OA to form the indium oleate complex. When using TOA solely, the small nanoparticles were grown (Fig. S3a,b). These results show that only in the ionic liquid solvent the TS  $\text{In}_2\text{O}_3$  or octahedral  $\text{In}_2\text{O}_3$  with polar surface is successfully prepared.

Because the {211} facets have high-density atom steps, ledges, and dangling bonds, the as-synthesized TS  $\text{In}_2\text{O}_3$  particles are anticipated to show good performance in gas sensing. In our experiments, ethanol was used as probe molecule to investigate gas-sensing properties of the samples, and the octahedron-shaped  $\text{In}_2\text{O}_3$  with exposed {111} facets was used as reference for comparison. Before the measurement, the sensors were calcined at 400 °C for 6 h to achieve stabilization and remove organic absorbents. Gas-sensing performance is also affected by the surface area, and a larger surface area usually results in better sensing properties. Therefore, in order to more clearly show the influence of the surface structure, the gas-sensing efficiencies were normalized by the BET surface areas of the TS  $\text{In}_2\text{O}_3$  particles (9.65  $\text{m}^2/\text{g}$ ) and the octahedron-shaped  $\text{In}_2\text{O}_3$  particles (7.76  $\text{m}^2/\text{g}$ ). In the gas sensing tests, all the  $\text{In}_2\text{O}_3$  samples had the same weight for convenience of comparison. Fig. 3a shows that the sensitivity of the TS  $\text{In}_2\text{O}_3$  particles is much higher than the octahedron-shaped  $\text{In}_2\text{O}_3$  particles. For example, at an ethanol concentration of 600 ppm, the sensitivity of the TS  $\text{In}_2\text{O}_3$  particles is about three times higher than the octahedron-shaped  $\text{In}_2\text{O}_3$  particles. The results indicate that the superior gas-sensing performance of the TS  $\text{In}_2\text{O}_3$  particles is not due to the surface area, but correlated with the surface structure of high-index facets which have high-density atom steps, ledges, and dangling bonds. To further study the thermal stability cycle of the sensors, the sensors have been heated on the gas sensing device for five days, the sensitive of the sensor has been measured once a day (24 h). Fig. 3b shows the TS  $\text{In}_2\text{O}_3$  sensor exhibits good thermal stability.

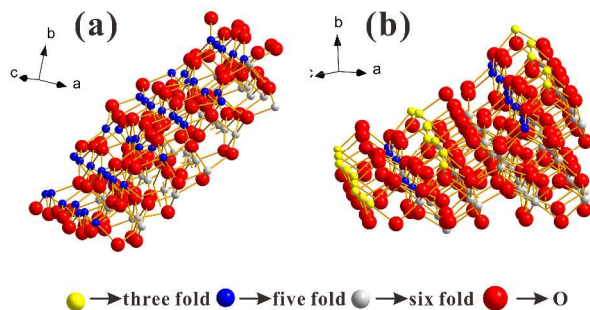


Fig. 4 Representation of the surface atoms model of (a) the {111} facets; (b) the {211} facets.

Fig. 4 shows the representative surface atoms model of  $\text{In}_2\text{O}_3$  {211} and {111} surfaces that contain several atom steps. For cubic phase  $\text{In}_2\text{O}_3$ , indium atoms in the bulk are sixfold-

coordinated by O atoms. At the surface, indium atoms are coordinative unsaturated. As shown in Fig. 4a, the cubic  $\text{In}_2\text{O}_3$  {111} surface contains rows of fivefold-coordinated indium atoms (blue) with one dangling bond perpendicular to the surface. However, on the {211} surface, all indium atoms are coordinative unsaturated, locating in fivefold-coordinated sites (blue) with one dangling bond and threefold-coordinated sites (yellow) with three dangling bonds (Fig. 4b). Therefore, there are more dangling bonds on the {211} surface than on the {111} surface. This indicates that for adsorption of ionized oxygen species, the {211} facets of  $\text{In}_2\text{O}_3$  is more active than {111} facets. At the same time, the {211} surface is a stepped surface composed of {111} terraces and (100) steps, which will further improve the activity of  $\text{In}_2\text{O}_3$  for adsorption of ionized oxygen species. The discussion above explain the result that the TS  $\text{In}_2\text{O}_3$  particles with exposed {211} facets exhibit higher gas sensing activity than octahedral  $\text{In}_2\text{O}_3$  particles with exposed {111} facets.

In conclusion, TS  $\text{In}_2\text{O}_3$  particles with exposed high-index {211} facets were synthesized by a simple wet chemistry route with the assistance of OA and TOA. The ionic liquid and the reaction temperature are the mainly influencing factors to synthesize the TS  $\text{In}_2\text{O}_3$  particles. Our results demonstrate that TS  $\text{In}_2\text{O}_3$  particles with exposed high-index {211} facets perform the high gas sensing activity and high thermal stability. In addition, the present study motivates us to further explore new synthetic methods for the preparation of other metal oxides with a high percentage of reactive facets, which have promising application as gas sensor, photocatalysis, optoelectronic devices, and solar cells.

This work was supported by the National Natural Science Foundation of China (Grant No. 21201088, 21333008, 21473081), the Qing Lan Project and the Project Funded by the Priority Academic Program Development of Jiangsu Higher Education Institutions.

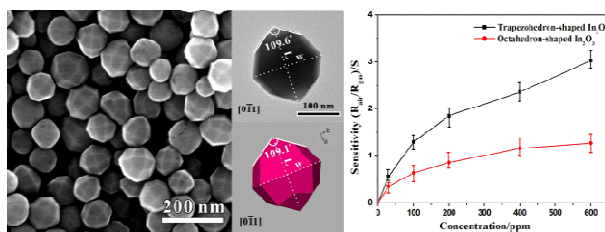
## References

- (a) A. R. Tao, S. Habas, P. Yang, *Small*, 2008, **4**, 310-325; (b) Z. Y. Jiang, Q. Kuang, Z. X. Xie, L. S. Zheng, *Adv. Func. Mater.*, 2010, **20**, 3634-3645; (c) M. H. Huang, S. Rej, S. Hsu, *Chem. Commun.*, 2014, **50**, 1634-1644.
- (a) N. Tian, Z. Y. Zhou, S. G. Sun, Y. Ding, Z. L. Wang, *Science*, 2007, **316**, 732-735; (b) T. Ming, W. Feng, Q. Tang, F. Wang, L. Sun, J. Wang, C. Yan, *J. Am. Chem. Soc.*, 2009, **131**, 16350-16351; (c) J. Zhang, M. R. Langille, M. L. Personick, K. Zhang, S. Li, C. A. Mirkin, *J. Am. Chem. Soc.*, 2010, **132**, 14012-14014; (d) Y. Yu, Q. Zhang, X. Lu, J. Y. Lee, *J. Phys. Chem. C*, 2010, **114**, 11119-11126; (e) N. Tian, Z. Y. Zhou, N. F. Yu, L. Y. Wang, S. G. Sun, *J. Am. Chem. Soc.*, 2010, **132**, 7580-7581; (f) Y. Yu, Q. Zhang, B. Liu, J. Y. Lee, *J. Am. Chem. Soc.*, 2010, **132**, 18258-18265; (g) T. Yu, D. Y. Kim, H. Zhang, Y. Xia, *Angew. Chem. Int. Ed.*, 2011, **50**, 2773-2777; (h) J. Xiao, S. Liu, N. Tian, Z. Y. Zhou, H. X. Liu, B. B. Xu, S. G. Sun, *J. Am. Chem. Soc.*, 2013, **135**, 18754-18757; (i) X. L. Xu, X. Zhang, H. Sun, Y. Yang, X. P. Dai, J. S. Gao, X. Y. Li, P. F. Zhang, H. H. Wang, N. F. Yu, S. G. Sun, *Angew. Chem. Int. Ed.*, 2014, **53**, 12522-12527; (j) X. G. Han, M. S. Jin, S. F. Xie, Q. Kuang, Z. Y. Jiang, Y. Q. Jiang, Z. X. Xie, L. S. Zheng, *Angew. Chem. Int. Ed.*, 2009, **48**, 9180-9183; (k) D. Fan, P. J. Thomas, P. O'Brien, *J. Am. Chem. Soc.*, 2008, **130**, 10892-10894; (l) L. H. Hu, Q. Peng, Y. D. Li, *J. Am. Chem. Soc.*, 2008, **130**, 16136-16137; (m) J. Yin, Z. Yu, F. Gao, J. Wang, H. Pang, Q. Lu, *Angew. Chem. Int. Ed.*, 2010, **49**, 6328-6332; (n) M. Leng M. Liu, Y. Zhang, Z. Wang, C. Yu, X. Yang, H. Zhang, C. Wang, *J. Am. Chem. Soc.*, 2010, **132**,

- 17084-17087; (o) M. R. Gao, Z. Y. Lin, J. Jiang, H. B. Yao, Y. M. Lu, Q. Gao, W. T. Yao, S. H. Yu, *Chem. Eur. J.* 2011, **17**, 5068-5075; (p) R. M. Liu, Y. W. Jiang, H. Fan, Q. Y. Lu, W. Du, F. Gao, *Chem. Eur. J.* 2012, **18**, 8957-8963; (q) Q. Kuang, X. Wang, Z. Y. Jiang, Z. X. Xie, L. S. Zheng, *Acc. Chem. Res.* 2014, **47**, 308-318.
- 5 (3) M. Curreli, C. Li, Y. Sun, B. Lei, M. A. Gundersen, M. E. Thompson, C. Zhou, *J. Am. Chem. Soc.*, 2005, **127**, 6922-6923.
- (4) D. Liu, W. Lei, S. Qin, L. Hou, Z. Liu, Q. Cuid, Y. Chen, *J. Mater. Chem. A* 2013, **1**, 5274-5278.
- 10 (5) A. Shanmugasundaram, B. Ramireddy, P. Basak, S. V. Manorama, S. Srinath, *J. Phys. Chem. C*, 2014, **118**, 6909-6921.
- (6) (a) Q. Tang, W. Zhou, W. Zhang, S. Ou, K. Jiang, W. Yu, Y. Qian, *Cryst. Growth. Des.*, 2005, **5**, 147-150; (b) G. Wang, J. Park, D. Wexler, M. S. Park, J. H. Ahn, *Inorg. Chem.*, 2007, **46**, 4778-4780;
- 15 (c) A. Vomiero, S. Bianchi, E. Comini, G. Faglia, M. Ferroni, G. Sberveglieri, *Cryst. Growth. Des.*, 2007, **7**, 2500-2504; (d) Z. Zhuang, Q. Peng, J. Liu, X. Wang, Y. Li, *Inorg. Chem.*, 2007, **46**, 5179-5187; (e) W. Lu, Q. Liu, Z. Sun, J. He, C. Ezeolu, J. Fang, *J. Am. Chem. Soc.*, 2008, **130**, 6983-6991; (f) Y. Liu, W. Yang, D.
- 20 Hou, *Superlattice. Microst.*, 2008, **43**, 93-100; (g) J. Yang, C. Li, Z. Quan, D. Kong, X. Zhang, P. Yang, J. Lin, *Cryst. Growth. Des.*, 2008, **8**, 695-699; (h) D. Caruntu, K. Yao, Z. Zhang, T. Austin, W. Zhou, C. J O'Connor, *J. Phys. Chem. C*, 2010, **114**, 4875-4886; (i)
- 25 X. M. Xu, P. L. Zhao, D. W. Wang, P. Sun, L. You, Y. F. Sun, X. S. Liang, F. M. Liu, H. Chen, G. Y. Lu, *Sensors and Actuators B*, 2013, **176**, 405- 412; (j) M. Meng, X. L. Wu, X. B. Zhu, L. Yang, Z. X. Gan, X. S. Zhu, L. Z. Liu, Paul K. Chu, *J. Phys. Chem. Lett.*, 2014, **5**, 4298-4304.
- (7) X. Zhou, Z. X. Xie, Z. Y. Jiang, Q. Kuang, S. H. Zhang, T. Xu, R. B. Huang, L. S. Zheng, *Chem. Commun.*, 2005, 5572-5574.
- 30

*Graphical Abstract*

The trapezohedraon-shaped (TS)  $\text{In}_2\text{O}_3$  particles with exposed high-index  $\{211\}$  facets were successfully synthesized in oleic acid (OA) and trioctylamine (TOA) system. It has been demonstrated that the gas sensing activity of TS  $\text{In}_2\text{O}_3$  particles with exposed high-index  $\{211\}$  facets is higher than that of octahedron-shaped  $\text{In}_2\text{O}_3$  particles with exposed low-index  $\{111\}$  facets.



5